

Pump power dependence of femtosecond two-color optical Kerr shutter measurements

Lihe Yan, Jinhai Si,* Yaqi Yan, Feng Chen, and Xun Hou

Key Laboratory for Physical Electronics and Devices of the Ministry of Education & Shaanxi Key Lab of Information Photonic Technique, School of Electronics & Information Engineering, Xi'an Jiaotong University, Xianning-xilu 28, Xi'an, 710049, China

*jinhaisi@mail.xjtu.edu.cn

Abstract: We investigated the pump power dependence of femtosecond two-color optical Kerr shutter (OKS) signals, which showed a damped sinusoidal variation with increasing pump power. The sinusoidal dependence was attributed to the polarization rotation caused by light-induced birefringence effect. The numerical analysis indicated that, the damping of OKS signal intensity could be attributed to the temporal profile change of probe pulse passing through the OKS setup, due to the non-uniform transient refractive index change induced by pump pulse. Because of the large phase shift of probe pulse, the time-resolved OKS signals showed modulated temporal intensity when pump power was increased.

©2011 Optical Society of America

OCIS codes: (320.7100) Ultrafast measurements; (320.5540) Pulse shaping; (320.7110) Ultrafast nonlinear optics; (320.2250) Femtosecond phenomena.

References and links

1. R. Righini, "Ultrafast optical Kerr effect in liquids and solids," *Science* **262**(5138), 1386–1390 (1993).
2. Y. Liu, F. Qin, Z. Y. Wei, Q. B. Meng, D. Z. Zhang, and Z. Y. Li, "10 fs ultrafast all-optical switching in polystyrene nonlinear photonic crystals," *Appl. Phys. Lett.* **95**, 13116–3 (2009).
3. D. G. Kong, W. B. Duan, X. R. Zhang, C. Y. He, Q. Chang, Y. X. Wang, Y. C. Gao, and Y. L. Song, "Ultrafast third-order nonlinear optical properties of $\text{ZnPc}(\text{OBu})_6(\text{NCS})/\text{DMSO}$ solution," *Opt. Lett.* **34**(16), 2471–2473 (2009).
4. H. W. Lee, J. K. Anthony, H. D. Nguyen, S. I. Mho, K. Kim, H. Lim, J. Lee, and F. Rotermund, "Enhanced ultrafast optical nonlinearity of porous anodized aluminum oxide nanostructures," *Opt. Express* **17**(21), 19093–19101 (2009).
5. J. Takeda, K. Nakajima, S. Kurita, S. Tomimoto, S. Saito, and T. Suemoto, "Time-resolved luminescence spectroscopy by the optical Kerr-gate method applicable to ultrafast relaxation processes," *Phys. Rev. B* **62**(15), 10083–10087 (2000).
6. L. Gundlach and P. Piotrowiak, "Femtosecond Kerr-gated wide-field fluorescence microscopy," *Opt. Lett.* **33**(9), 992–994 (2008).
7. T. Yasui, K. Minoshima, and H. Matsumoto, "Three-dimensional shape measurement of a diffusing surface by use of a femtosecond amplifying optical Kerr gate," *Appl. Opt.* **39**(1), 65–71 (2000).
8. L. Wang, P. P. Ho, C. Liu, G. Zhang, and R. R. Alfano, "Ballistic 2-d imaging through scattering walls using an ultrafast optical Kerr gate," *Science* **253**(5021), 769–771 (1991).
9. R. A. Ganeev, A. I. Rysanyansky, M. Baba, M. Suzuki, N. Ishizawa, M. Turu, S. Sakakibara, and H. Kuroda, "Nonlinear refraction in CS_2 ," *Appl. Phys. B* **78**(3–4), 433–438 (2004).
10. B. L. Yu, H. P. Xia, C. S. Zhu, and F. X. Gan, "Enhanced third-order nonlinear optical properties of C_{60} -silane compounds," *Appl. Phys. Lett.* **81**(15), 2701–2703 (2002).
11. H. Z. Tao, G. P. Dong, Y. B. Zhai, H. T. Guo, X. J. Zhao, Z. W. Wang, S. S. Chu, S. F. Wang, and Q. H. Gong, "Femtosecond third-order optical nonlinearity of the $\text{GeS}_2\text{-Ga}_2\text{S}_3\text{-CdI}_2$ new chalcogenide glasses," *Solid State Commun.* **138**(10–11), 485–488 (2006).
12. T. X. Lin, Q. Yang, J. H. Si, T. Chen, F. Chen, X. L. Wang, X. Hou, and K. Hirao, "Ultrafast nonlinear optical properties of $\text{Bi}_2\text{O}_3\text{-B}_2\text{O}_3\text{-SiO}_2$ oxide glass," *Opt. Commun.* **275**(1), 230–233 (2007).
13. H. Kanbara, H. Kobayashi, T. Kaino, T. Kurihara, N. Ooba, and K. Kubodera, "Highly efficient ultrafast optical Kerr shutters with the use of organic nonlinear materials," *J. Opt. Soc. Am. B* **11**(11), 2216–2223 (1994).
14. Y. Kondo, H. Inouye, S. Fujiwara, T. Suzuki, T. Mitsuyu, T. Yoko, and K. Hirao, "Wavelength dependence of photoreduction of Ag^+ ions in glasses through the multiphoton process," *J. Appl. Phys.* **88**(3), 1244–1250 (2000).
15. P. P. Ho and R. R. Alfano, "Optical Kerr effect in liquids," *Phys. Rev. A* **20**(5), 2170–2187 (1979).
16. E. P. Ippen and C. V. Shank, "Picosecond response of a high-repetition-rate CS_2 optical Kerr gate," *Appl. Phys. Lett.* **26**(3), 92–93 (1975).

17. A. Brodeur and S. L. Chin, "Ultrafast white-light continuum generation and self-focusing in transparent condensed media," *J. Opt. Soc. Am. B* **16**(4), 637–650 (1999).
18. J. Etchepare, G. Grillon, J. P. Chambaret, G. Hamoniaux, and A. Orszag, "Polarization selectivity in time-resolved transient phase grating," *Opt. Commun.* **63**(5), 329–334 (1987).

1. Introduction

For the last few decades, femtosecond optical Kerr shutter (OKS) technique has been developed as a key tool to measure the nonlinear response of all kinds of materials [1–4]. As the femtosecond OKS technique provides an ultrafast measurement of high speed, broad wavelength range, ultrafast switching time, and high precision, it has been widely used to investigate the ultrafast fluorescence spectroscopy, high time-resolved imaging, ballistic light imaging, and etc [5–8]. As the key factor to construct an OKS configuration, a suitable Kerr medium should be of a large nonlinearity and ultrafast nonlinear response. CS₂ has been widely used as the Kerr medium because of its strong nonlinear response and easy access, and has been often selected as the reference sample in the OKS measurements [9–15].

In the optical Kerr effect, the pump light passing through the nonlinear material will induce a birefringence in the sample. When the probe light passing through the same material, a phase shift occurs between its components polarized parallel and perpendicular to pump light field, which can be expressed by [13, 14]:

$$\Delta\phi = 2\pi n_2 L_{\text{eff}} I_g / \lambda_p \quad (1)$$

Here, n_2 is the nonlinear refractive index, while L_{eff} , λ_p and I_g denotes the effective length, wavelength of the probe light, and pump intensity, respectively. The OKS signal intensity passing through the polarizer behind the Kerr medium is given by [13, 14]:

$$I_{\text{OKS}} = I_{\text{probe}} \sin^2(2\theta) \sin^2(\Delta\phi/2) \quad (2)$$

Here, I_{probe} is the probe beam intensity and θ is the polarization angle between pump and probe beams. One could expect that the transmittance of the OKS setup should vary sinusoidally as a function of pump power. As the phase shift was probably very small, the OKS signals measured in the previous reports generally showed quadratic pump power dependence [10, 13, 14].

In the OKS measurements, the time-dependent phase shift is a time convolution of the pump pulse and the nonlinear response function of Kerr medium. In the picosecond regime, since the response time of CS₂ is faster than the pulse duration, temporal behavior of the nonlinear phase change essentially follows the shape of the laser pulse, and the time-resolved OKS signals is mainly determined by the pulse duration [15]. However, in the femtosecond regime, if the duration time of the probe pulse is close to the response time of CS₂, the probe pulse will experience a time-dependent birefringence resulting in a time-dependent polarization. As a result, damped sinusoidal pump intensity dependence might occur, due to the temporal profile change of the OKS signals.

In this paper, we investigated the pump power dependence of femtosecond two-color OKS experiments in CS₂, which showed a damped sinusoidal variation. To understand the damping of the peak intensity of the pump power dependence, we simulated the probe pulse profile change after passing through the OKS setup. The numerical analysis indicated that, the damping of the OKS signal intensity could be attributed to the temporal profile change of probe pulse, which was caused by the non-uniform transient refractive index change induced by pump pulse. The time-resolved OKS signals showed modulated temporal intensity when the pump power was increased.

2. Experiments

In our experiments, a femtosecond two-color pump-probe OKS arrangement was employed. The experimental setup used was similar to that reported elsewhere [12], except that a second harmonic was used as the probe light. Briefly, the output of laser system was 30 fs pulses

centered at 800 nm at a repetition rate of 1 kHz. The laser beam was split into two beams, one of which was used as the pump beam and the other beam was passed through a 1-mm thick type-I-BBO crystal generating 50 μW second harmonic as the probe light. The duration of the 400 nm probe pulse was estimated to be about 300 fs. The pump pulse passed through a time delay line and a $\lambda/2$ plate to control the delay and polarization angle between the pump and probe pulses, respectively. Both the two beams were focused by lenses and then incident into the 1 mm sample cell filled with CS_2 at an interaction angle of 12° . To avoid the white-light continuum, the pump power was kept below 10 mW [17].

3. Results and discussion

3.1 Pump power dependence of the femtosecond two-color OKS signals

In the OKS measurements, the probe light field transmitted through the polarizer, as a function of the delay time τ between the pump and probe pulses is given by [1, 15, 16]:

$$I_{oks}(t, \tau) \propto I_{probe}(t - \tau) \cdot \sin^2 \left[A \int_{-\infty}^t R(t - t') \cdot I_g(t') dt' \right] \quad (3)$$

Here, the term in the square bracket denotes the phase shift $\Delta\phi(t)/2$ for $I_{probe}(t)$ caused by birefringence effect. A is a constant, and $R(t)$ is the normalized response function of the sample. If the pump pulse duration is short enough comparing with that of the probe light, it can be approximated as an instantaneous delta function. Based on this assumption, when the delay τ between the two incident pulses is set 0, Eq. (3) can be simplified as:

$$I_{oks}(t) \propto I_{probe}(t) \cdot \sin^2 [A I_g \cdot R(t)] \quad (4)$$

The probe pulse will experience a time-dependent birefringence resulting in a time-dependent polarization. As a result, the temporal profile of the probe pulse passed through the polarizer will be changed, and the visibility of the probe pulse could be significantly reduced. Hence, damped sinusoidal pump intensity dependence might occur at high pump powers, under which a large phase shift might be induced.

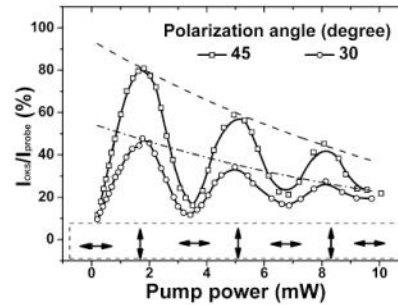


Fig. 1. Pump power dependence of OKS signals in CS_2 when the polarization angle between the pump and probe beams was fixed at 45° and 30° , respectively. The arrows in the rectangle show the polarization directions of the OKS signals at the corresponding pump power. The dashed lines (guided for eyes) show the attenuation trend of peak intensity.

Figure 1 shows the pump power dependence of the OKS signals for CS_2 , when the delay time between the pump and probe pulses was fixed at 0. The squares and circles in Fig. 1 indicate the OKS signals intensity as a function of the pump power, when the polarization angles between the two beams were fixed at 30° and 45° , respectively. As shown in Fig. 1, when the pump power was adjusted to about 1.7 mW, the polarization plane of the probe pulse was rotated by $\pi/2$ and the probe pulse could pass through the analyzer. When the pump power was further increased, the probe pulse would be depolarized again, and would become linearly polarized with the polarization plane rotating π when the pump power was fixed at about 3.3 mW. With the pump power further increasing, the rest might be deduced by

analogy. We can deduce the value of constant A using Eq. (4), which was calculated to be about $1.54 \times 10^{-10} \text{ cm}^2/\text{W}$. The arrows in the dashed rectangle in the bottom of Fig. 1 show the polarization plane change of the probe light at the corresponding pump power. The pump power dependence of the OKS signals showed an obvious damped sinusoidal variation, which was mainly attributed to the temporal profile change of probe pulse passing through the OKS setup. The dashed and dash-dotted lines in Fig. 1 show the attenuation trend of the peak intensity guided for eyes when the polarization angle was fixed at 45° and 30° , respectively.

In our experiments, the 400 nm probe pulse was temporally broadened comparing with the 800 nm pump pulse. The incident probe pulse duration was measured by OKS measurement, with a 1 mm thick fused silica as the Kerr medium. The dotted line in Fig. 2(a) shows the temporal profile of 400 nm pulse $I_{probe}(t)$, the full-width of half-maximum (FWHM) of which was evaluated to be about 300 fs. As the pump pulse was short enough comparing with the nonlinear response of CS_2 , it can be approximated as an instantaneous delta function. The nonlinear response function $R(t)$ of the sample was characterized by the time-resolved degenerated OKS signals with the pump and probe pulses at 800 nm in CS_2 , as shown by the solid line in Fig. 2(a). The result indicated that the nonlinear response of CS_2 was mainly attributed to molecular response, which could be well fitted using the law given by J. Etchepare et al. [18].

Because of the transient nonlinear response of the material, the probe light field might experience the building and relaxation processes of the nonlinear response within the pulse duration region. Due to the non-uniform refractive index change of the Kerr medium, each part of the probe pulse had different transmittance. The intensity of the probe light field passing through the OKS setup $I_{oks}(t)$ was calculated using Eqs. (3) and (4). According to our experimental results, the maximal transmittance of the OKS configure occurred when the pump power was adjusted to be about $1.7 \times (2n-1) \text{ mW}$ ($n=1, 2, 3, \dots$), where the polarization plane of the probe light was rotated by $(2n-1)\pi/2$ ($n=1, 2, 3, \dots$). The solid lines in Fig. 2 (b)-(d) show the simulated probe pulse profile after passing through the OKS setup, when the pump power was fixed at 1.7 mW, 5.1 mW, 8.4 mW, respectively. The dotted lines in Fig. 2 (b)-(d) show the incident probe pulse profile $I_{probe}(t)$.

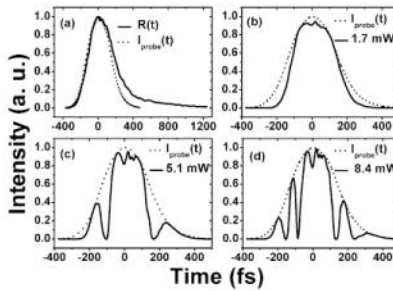


Fig. 2. (a) Temporal profile of 400 nm probe pulse $I_{probe}(t)$ and nonlinear response of CS_2 $R(t)$, and temporal profile of the probe pulse after passing through the OKS setup when the pump power was fixed at (b) 1.7 mW, (c) 5.1 mW, and 8.4 mW, respectively. The dashed lines in (b)-(d) show the temporal profiles of the incident probe pulse $I_{probe}(t)$.

The simulated results indicated that the probe pulse profiles were changed after passing through the OKS setup. When the pump power was fixed at 1.7 mW, the phase shift $\Delta\phi$ for the very peak of the pulse $I_{probe}(t=0)$ was estimated to be π , while that for the trailing and leading parts of the pulse was smaller. Hence, the transmittance of the pulse became smaller from the peak to the both side edges, as shown by the solid line in Fig. 2(b). When the pump

power was adjusted to 5.1 mW, the phase change for the light field at the peak $I_{probe}(t=0)$ was calculated to be 3π . However, when the phase shift for the light field at both sides was decreased to π , the light field was able to pass through the OKS setup again. As shown Fig. 2(c), the transmitted probe pulse showed a triple-peak profile. Figure 2(d) shows the probe pulse profile, when the pump power was fixed at 8.5 mW. The transmitted pulse showed an even more complex profile with two “wings” on each shoulder.

As what we detected in the experiments was the energy of the probe light passing through the analyzer, we integrated the incident probe pulse as well as the transmitted pulses with respect to time. The solid, dashed, dotted and dash-dotted lines in Fig. 3 show the integrations of the intensity for the incident pulse and the transmitted pulses when the pump power was fixed at 1.7 mW, 5.1 mW, and 8.5 mW, respectively. The inset shows the final values of the integrations of the pulses which were shown in Fig. 2(b)-(d). The simulated results showed an obvious damping with increasing pump power, agreeing well with our experimental results.

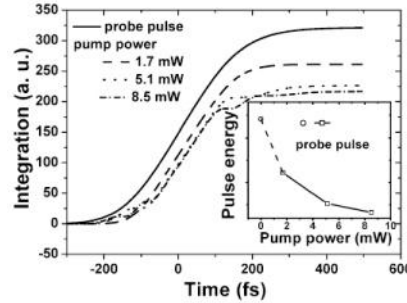


Fig. 3. Integrations of the intensity of the incident probe pulse and the pulse after passing through the analyzer, when the pump power was fixed at 1.7 mW, 5.1 mW, and 8.5 mW, respectively. The inset in (b) shows the integration results of the transmitted pulse as well as the incident probe pulse.

3.2 Femtosecond time-resolved OKS signals in CS_2

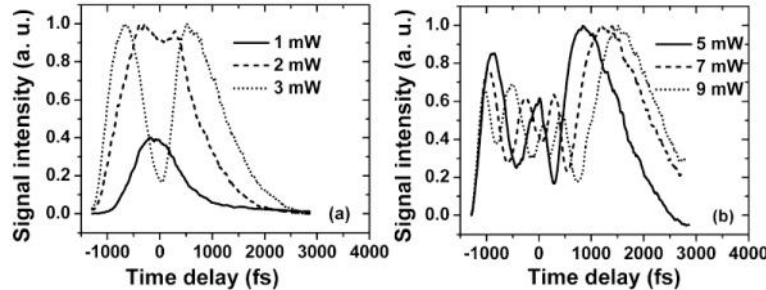


Fig. 4. Time-resolved OKS signals in CS_2 , when pump power was fixed at (a) 1 mW, 2 mW, and 3 mW, and (b) 5 mW, 7 mW, and 9 mW, respectively.

According to Eqs. (3) and (4), the time-resolved OKS signal as a function of the delay time is:

$$S(\tau) \propto \int_{-\infty}^{\infty} I_{probe}(t-\tau) \cdot \sin^2 [AR(t-t) \cdot I_g(t)] dt \quad (5)$$

Hence, the probe pulse will experience time-dependent birefringence at different delay times, and modulated temporal intensity of the time-resolved OKS signals might be exhibited. The solid, dashed, and dotted lines in Fig. 4(a) show the time-resolved OKS signals of CS_2 when the pump power was fixed at 1 mW, 2 mW, and 3 mW, respectively. When the pump power was fixed at 1 mW, the time-resolved OKS signals showed a normal profile with a relaxation time of 1.5 ps [9]. When the pump power was adjusted to 2 mW, the signal profile showed a saturated curve, as shown by the dashed line. When the pump power was increased

to be about 3 mW, the probe pulse would experience phase shift as large as about 2π . However, when the probe pulse was delayed from the pump pulse, the probe pulse would experience the rising and relaxation processes of the nonlinear response of the medium, and the probe light field would experience a smaller phase shift than that at 0 delay time. Hence, the temporal profile of the OKS signal showed a peak-valley-peak pattern. As shown by the dotted line in Fig. 4(a), the former peak showed a symmetric profile and the latter one showed a slow relaxation behavior, which corresponds to the building process and relaxation process, respectively. The solid, dashed, and dotted lines in Fig. 4(b) show the time-resolved OKS signals of CS₂ when the pump power was fixed at 5 mW, 7 mW, and 9 mW, respectively. At higher pump powers, multi-peak OKS signal profiles was observed. As denoted by the arrows in the rectangle in Fig. 1, the polarization plane could be rotated by about $3\pi/2$, 2π , and $5\pi/2$, when the pump power was fixed about 5 mW, 7 mW, and 9 mW, respectively.

3.3 Polarization dependence of the femtosecond two-color OKS signals

To further understand the origin of the OKS signals, we measured the dependence of the OKS signal intensity on the polarization angle between the pump and probe beams. The squares and circles in Fig. 5 show the polarization dependence of the OKS signals, when the delay time was fixed at 0 and the pump power fixed at 1 mW and 5 mW, respectively. The solid and dashed lines in Fig. 5 show the fitted curve of the polarization dependence of the OKS signals using Eq. (2). The curves showed a period of $\pi/2$, with the maximum and minimum values occurring at $n\pi/2 + \pi/4$ and $n\pi/2$ ($n=0,1,2,\dots$) respectively. Hence, the OKS signals were attributed to light-induced birefringence effect in our experiments.

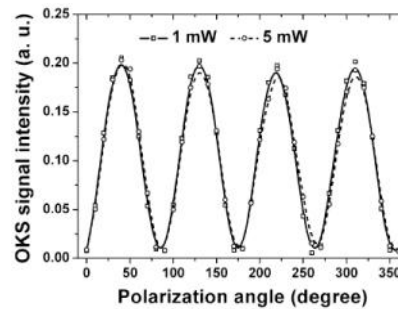


Fig. 5. Polarization dependence of OKS signals in CS₂, when the delay time was kept at 0 and the pump power was adjusted to 1 mW and 5 mW, respectively.

4. Conclusions

In conclusion, we investigated the pump power dependence of two-color femtosecond OKS signal. The OKS signals showed a damped sinusoidal dependence on the pump power, which was attributed to the polarization direction change of the probe pulse caused by the light-induced birefringence effect. The damping of the amplitudes was attributed to the temporal profile change of probe pulse, due to the non-uniform transient refractive index change caused by pump pulse. Due to the refractive index change induced by the pump beam, the time-resolved OKS signals showed modulated temporal intensity when the pump power was increased. The polarization dependence indicated that the OKS signals were attributed to light-induced birefringence effect.

Acknowledgments

The authors gratefully acknowledge the financial support for this work provided by the National Science Foundation of China (Grant No.11074197) and the Specialized Research Fund for the Doctoral Program of Higher Education of China (Grant No. 200806980022).